HHS Public Access

Author manuscript

Sens Actuators A Phys. Author manuscript; available in PMC 2020 May 01.

Published in final edited form as:

Sens Actuators A Phys. 2019 May 1; 290: 130–136. doi:10.1016/j.sna.2019.03.028.

A One-step Residue-free Wet Etching Process of Ceramic PZT for Piezoelectric Transducers

Haoran Wang[1], **Manish Godara**[2], **Zhenfang Chen**[3], and **Huikai Xie**[1,4]

[1]Department of Electrical and Computer Engineering, University of Florida, Gainesville, USA

[2]Department of Chemical Engineering, University of Florida, Gainesville, USA

[3]MEMS Engineering and Materials Inc., Sunnyvale, USA

[4]School of Information and Electronics, Beijing Institute of Technology, Beijing, China

Abstract

Lead zirconate titanate (PZT) has wide applications in microelectromechanical systems (MEMS) due to its large piezoelectric coefficients. However, there exist serious issues during PZT wet etching even with multiple etching steps, such as residues on etching fronts and large undercut. In this paper, a one-step residue-free wet etching process of ceramic PZT is developed with fluoroboric acid. In this work, the design of experiments (DOE) method is employed to minimize undercut and residues without sacrificing etching rate. The acid concentration, temperature, and agitation are the process parameters considered in the DOE. Through DOE analysis of the experimental data, an optimal recipe is identified as the volume ratio of HBF_4:H_2O=1:10 at 23 °C. This new PZT etching recipe leads to a high etching rate (1.54 μm/min) with no observable residues and a small undercut (0.78:1) as well as a high selectivity over the photoresist (900:1). This etching recipe can be used for making various piezoelectric transducers.

Graphical Abstract

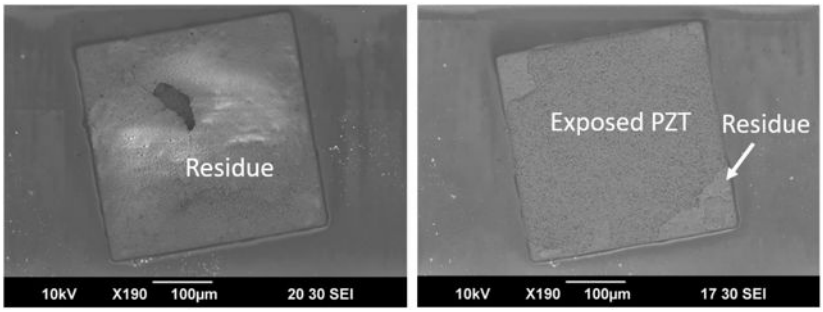

Most of PZT wet etching recipes form residues and ultrasonic cleaning is applied, which is not suitable for ceramic PZT with multi-layer structures.

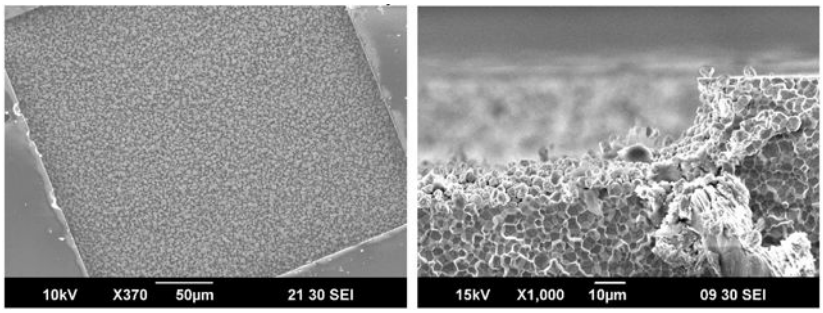

A one-step residue-free recipe without using ultrasonic agitation is developed. The optimal recipe with proper etch rate, small undercut and high selectivity to the mask material was found using Taguchi design of experiments (DOE) method.

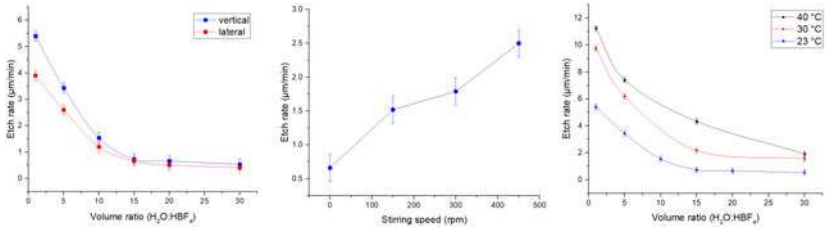

Etch rates with different acid concentrations, stirring speeds and temperatures were experimentally obtained and plotted, which can be adopted for different etching purposes.

Keywords

PZT; ceramic PZT; PZT transducers; wet etching; residue-free; HBF_4

I. Introduction

Piezoelectric materials can be used in a wide range of applications, including RF filters [1], actuators [2][3], ultrasonic motors [4], acoustic generators [5][6] and acoustic sensors [7]. In recent years, with the advancement of piezoelectric thin-film technologies, piezoelectric MEMS devices draw a lot of attention from both academia and industry. Various piezoelectric materials, including ZnO [8], PVDF [9], PZT [10] and A1N [11], have been integrated and micromachined to manufacture ultrasonic transducers, loudspeakers, and bulk acoustic wave resonators. Among them, PZT is particularly at the spot of interest due to its high piezoelectric coefficients and good electromechanical coupling. PZT thin films are typically fabricated by sol-gel processing or sputtering [12][13]. It was also reported that ceramic PZT, bonded on silicon, could be thinned down to 26 µm [14]. Compared to thin-film PZT, ceramic PZT has almost four times higher piezoelectric constants and can provide larger electromechanical coupling, thus offering better performances in energy harvesters, microsensors and microactuators [15][16]. For example, Aktakka *et al.* presented a piezoelectric energy harvester based on 13 µm-thick ceramic PZT, demonstrating improved output voltage and higher power density [17], Wang *et al.* reported acoustic transducers fabricated by bonding and polishing ceramic PZT on an SOI wafer, provided a promising

approach to fabricate piezoelectric MEMS devices [18][19]. In all these cases, PZT etching is an essential fabrication step.

Both dry and wet etching methods of PZT have been studied and reported [20]-[22]. Dry etching processes, including ion beam etching (IBE) and reactive ion etching (RIE), have poor selectivity of PZT over the photoresist and metal electrode layers. Low etching rate and material redeposition on sidewalls are other limiting factors of the dry etching methods. There is also a contradiction between increasing the etch rate and keeping the stability of the photoresist [23]. In comparison, wet etching is a more effective method with high etching rate, low cost and high selectivity. However, since PZT is a compound consisting of lead, zirconium and titanium components, its etching process is quite complicated as multiple acids are usually needed. Insoluble by-products are formed in the chemical reaction, resulting in residues at the etching fronts. A few wet etching recipes have been reported in etching sol-gel PZT thin films, but most of the recipes have common issues such as serious residues and large undercut [22][24]. For example, Mancha *et al.* reported a BHF+HCl recipe with a PZT etch rate of 0.6 μm/min, but there existed heavy residues and a large undercut ratio (5.5:1, lateral undercut: depth) [24]. Zheng *et al.* further added NH_4Cl and reduced the undercut down to 1.5:1 [22], but residues remained.

To deal with the residue issue, an additional $2HNO_3$:$1H_2O$ etching step was added to remove residues [22]. Several other methods of residue removal were also reported, including a dip process in 70 °CDI water [25] and ultrasonic cleaning [26]. For ceramic PZT, Wang *et al.* tried six different wet-etching solutions and the results showed that the recipe consisting of BHF:HNO_3:HAC:H_2O_2:EDTA=1:2:2:1:2 was the optimal one with an undercut ratio of 1.31:1 [27]. However, insoluble residues still existed and must be removed by DI water after etching.

Almost all of the PZT wet etching processes reported in the literature require two processing steps [22][24]-[28], complicating the fabrication. Residues produced during etching may decrease or even stop the further etching and cause seriously nonuniform etching fronts. Moreover, ceramic PZT is usually bonded on the substrate using adhesives [14][17]-[19], forming multi-layer structures with polymer layers built in. As a result, the two-step etching recipes for sol-gel PZT that require ultrasonic cleaning may cause peel-off or delamination when applied to etch ceramic PZT in multi-layer structures. Thus, one-step PZT etching processes are needed, especially for ceramic PZT. One such attempt was reported by Che *etal.* using HNO_3: BHF: H_2O=4.5: 4.55: 90.95 to realize one-step wet etching of 1.0 μm-thick sol-gel PZT in only 20 seconds with ultrasonic agitation [29], where the undercut ratio was 1.1:1. However, when we applied this recipe except ultrasonic agitation to etch ceramic PZT with depths of more than 3 μm, heavy residues still appeared as the etching time needed was more than 3 minutes (See Section II).

In this study, a one-step etching recipe without ultrasonic agitation that works for ceramic PZT is developed. The recipe produces no residues, small undercut, modest etching rate and high selectivity. The paper is organized as follows. In Section II, we look into the problems when the popular two-step PZT etching recipes are applied to ceramic PZT. Section III introduces the new one-step etching recipe and the design of experiments (DOE) with

several process parameters considered. Section IV describes the ceramic PZT etching experiments. Section V shows the experiment results and discusses the etch rate, undercut and selectivity of this new wet etching process and their relationships with the acid concentration, temperature and agitation.

II. Two-step Etch of Ceramic PZT

Two popular PZT wet etching recipes were applied to etch ceramic PZT. The ceramic PZT was PZT-5H (CTS Corporation, USA). A recipe consisting of 4.5% BHF:4.55% HNO_3:90.95% H_2O was used to etch a ceramic PZT sample. No ultrasonic agitation was applied. The etching rate was 2.4 μm/min. As shown in Fig. 1(a), large residues were present during the etching. After dipped in 40°C DI water for 10 minutes, only a small amount of residues were removed (Fig. 1(b)). Even after rinsed with water gun for 2 minutes, there were still residues remained (Fig. 1(c)).

Another recipe consisting of BHF, HNO_3 and HCl with a volume ratio of 2:2:1 was prepared to etch another ceramic PZT sample. A mixture of 10 mL BHF, 10 mL HNO_3 and 5 mL HCl was diluted in 75 mL H_2O. The etching rate was about 0.7 μm/min. As shown in Fig. 2(a), there was still a residue issue. The residues covered a large portion of the to-be-etched PZT area, which may cause various problems. For example, the residues may significantly decrease the etching rate of the regions covered by them or even stop further etching, leading to poor etching uniformity. In addition, residues, if not removed, may lead to electrical contact issues. Ultrasonic cleaning was found to be effective to remove residues. As shown in Fig. 2(b), after a 10 seconds ultrasonic cleaning, over 80% residues were removed. Fig. 2(c) is a zoom-in SEM image showing the exposed and residue-covered regions in the etching cavity. However, using ultrasonic cleaning in the etching process has limitations, especially when dealing with multi-layer structures with polymer layers embedded or microstructures with suspensions or thin membranes.

The wet etching processes discussed above are two-step processes that still lead to residue issues in ceramic PZT etching. In this work, we will present a simple one-step wet etching process of ceramic PZT. Different from commonly used recipes containing BHF, HCl and HNO_3, only one acid is required in this new recipe. By using HBF_4, we found that ceramic PZT can be etched effectively without forming noticeable residues. In the following section, a design of experiment (DOE) technique is applied to study the etching rate, undercut, selectivity and residue under various etching conditions with HBF_4 etching PZT.

III. Design of Experiments

The goal is to develop an etching recipe that meets the three requirements in etching rate, selectivity and residue, which will be obtained by controlling three key parameters, i.e., acid concentration, temperature, and agitation. This requires a large number of experiments to find the optimal etching conditions. To minimize the number of experiments, Taguchi DOE method [30] is used in this study. This method creates orthogonal arrays based on different process parameters and their levels. Guided by the orthogonal arrays, the number of experiments will be greatly reduced and the influences of process variables will be easily

determined. In this work, the Taguchi DOE method is employed first to find the proper process parameters and determine the effects of those design parameters.

In the Taguchi analysis for this PZT wet etching, the design parameters include the fluoroboric acid concentration, temperature, and agitation of the etching. The concentration of the fluoroboric acid is expressed in the volume ratio between the coimnercial standard fluoroboric acid (50 wt.%) and DI water. Three levels are designed for each design parameter, as shown in Table I. The objectives of the experiment are to achieve proper etch rate (1–2 μm/min), small undercut ratio (<1), no residue, and high selectivity (> 500) to the mask material.

Based on Taguchi analysis, there are three independent design parameters (P=3) and each parameter has three levels (L=3). An L9 orthogonal array is applied and nine experiments are designed, as shown in Table II. A rotator (ImmunoMix, model 5090) with a rotation speed of around 90 rpm and an ultrasonic cleaning bath (Fisher Scientific Co., model: FS20D) were used for vibration and ultrasound agitation in the designed experiments.

Next, relationships between the etch rate and the acid concentration, the etchant temperature, and the stirring speed of the agitation were studied individually within a proper range. The acid was diluted at volume ratios (HBF_4:H_2O) of 1:1 to 1:30. The experimental setup is shown in Fig. 3. A stirring hotplate (Fisher Scientific Co., model: Fisher Scientific Isotemp) was used in this work to achieve the designed temperatures and stirring speeds. A temperature sensor was connected to the hotplate with its tip submerged in the liquid so that the etchant temperature was controlled in real time through the feedback. A magnetic stirrer was used to stir the liquid at the specific speeds. The stirring speed was controlled from 150 rpm to 450 rpm and the temperature effect was studied from room temperature (23 °C to 60 °C.

IV. Experiments

The ceramic PZT wafer (PZT 5H, CTS) used in this study had an initial thickness of 660 μm. It was first bonded on a silicon wafer by SU-8 photoresist, and then thinned down to about 100 μm with a grinding and chemical mechanical polishing process. After that, the thinned PZT wafer was cut into small samples with an area of 2 cm by 2 cm each. A cross-sectional view of a PZT sample is shown in Fig. 4, where the average PZT grain size was about 2.6 μm.

Various square patterns with dimensions ranging from 100 μm to 500 μm were designed. A 3.5 μm-thick photoresist (AZnLOF 2035) was coated, patterned, and hard baked at 112°C for 15 minutes as the etching mask. A few silicon samples were also prepared following the same procedure, used for studying the selectivity over the photoresist in the etching process.

For each etching experiment, the sample was etched for 1 minute first to exclude the surface effects of the PZT etching, and then etched for two cycles with 5 minutes on average (adjusted when etching was too fast or too low) for each cycle. The etch depth was then measured with a profilometer (Tencor AS500; KLA-Tencor, Milpitas, CA, USA) and the undercut was observed and measured with an SEM and an optical microscope. Also, the

SU-8 bonding was strong and no PZT layer peeling-off was observed during the experiments.

V. Results and Discussion

All experiments showed that there were no residues observed after the wet etching of the ceramic PZT samples with HBF_4. The etched patterns were inspected with an optical microscope and an SEM. As shown in Fig. 5, the etched pattern was clean and uniform without any residues. The actual chemical reactions and mechanism of HBF_4 etching PZT is out of the scope of this paper and will be investigated further.

The etching results of the experiments based on the Taguchi DOE are shown in Table III.

Table IV shows the mean values of each level of the different design parameters. Because the experiments were designed based on the orthogonal array, the mean values of each level at different design parameters can be easily calculated to evaluate the influences of those design parameters. For example, the etch rate data at the level 1 of the temperature is the mean value of all vertical etch rates at 23 °C in Table III, where S is defined as the standard deviation, calculated from all data of three levels at the specific design parameters. The larger the standard deviation, the stronger the influence of the corresponding design parameter is.

As shown in Table IV, the rank of the influence on the etching rate is agitation > volume ratio > temperature. However, this conclusion is relative to the three levels set for design parameters. From Tables III and IV, we found that with ultrasound agitation, both vertical etching rate and undercut increase significantly. For agitation, the effect of the level 3 (ultrasound) is much stronger than level 2 (vibration), which makes S larger. For instance, the 1:1 volume ratio recipe with ultrasonic agitation at 40 °C has an undercut of 19.2 μm/min. For volume ratio, we found that without any dilution, the etching rate of the PZT is low but the undercut is very high. Besides, high concentration acid attacks the photoresist and may even cause peel-off.

The selectivity over the photoresist was evaluated based on the patterned silicon samples. There was almost no change of the photoresist thickness on the silicon samples after dipped in the etching solutions for the same time with PZT samples. The photoresist was intact and there was not any peeling-off observed.

The effects of the volume ratio, stirring speed and temperature were studied individually in detail. Since ultrasound is a very strong agitation and it increases the etch rate significantly. Etching a thin PZT film with ultrasonic agitation is too fast and it is not desired. Instead, stirring is chosen as a moderate agitation in the experiments. The results are plotted in the following four figures, revealing that etching with a volume ratio of HBF_4:H_2O=1:10 at room temperature (23 °C is the optimal recipe with all design objectives achieved. Meanwhile, by controlling the acid concentration, temperature and stirring speed, various etch rates can be obtained for different etching purposes. As shown in Fig. 6, the etch rate decreases with the decreasing acid concentration while the undercut stays relatively constant between 0.6 and 0.8. As shown in Fig. 7, with a constant acid concentration (volume ratio of

HBF_4:H_2O=1:20), the etch rate increases with the increasing stirring speed. A volume ratio of 1:20 is chosen in this experiment because a small etch rate is needed as the start point to find out how much the etch rate is affected by increasing the stirring speed.

The influence of the temperature is shown in Fig. 8. The etch rate increases with the increasing temperature. Moreover, the etch rates at different temperatures under a volume ratio (HBF_4:H_2O) of 1:20 are shown in Fig. 9. By presenting the etch rate in the nature logarithm scale, it shows a linear trend between the etch rate and the inverse of the absolute temperature. The result shows that the etching process is a reaction limited process and has a strong dependence of the temperature. The linear fitted result is consistent with the relationship described in Arrhenius equation:

$$R = R_0 \exp(-E_a / kT) \quad (1)$$

where R is the rate constant, R_0 is the pre-exponential factor, E_a is the activation energy, k is the Boltzmann constant and T is the temperature.

As can be seen from Figs. 6-9, the etching rate and undercut are positively correlated with the acid concentration, agitation and temperature. Since a typical piezoelectric MEMS device usually has a PZT layer with a thickness less than 10 μm, an etching rate in the range of 1-2 μm/min is desired. Thus, HBF_4:H_2O=1:10 at 23 °C is an optimal recipe with all design objectives achieved (the etch rate is 1.54 μm/min, the undercut ratio is 0.78:1, and the selectivity is over 900 to the photoresist). Also, 23 °C is the room temperature, so setting up the experiment is easy. For etching thicker PZT, higher acid concentration, adding agitation, and/or increasing the temperature can be applied.

The surface profile of the etched patterns was observed with SEMs and also measured with a surface profilometer (Dektak 150, Veeco Instruments, Tucson, USA). One top-view and one cross-sectional SEM images of a moderately etched sample are shown in Fig. 10 (a)(b), exhibiting a smooth surface and a positive sidewall angle. Fig. 10 (c)(d) show an over etched sample with the PZT completely removed in the cavity and the SU-8 exposed. There were no residues observed on the over-etched sample. The measured surface profiles of a half-etched PZT cavity and an over-etched PZT cavity are plotted in Fig. 11, where the cavity is designed with a length of 500 μm. As it can be seen from Fig. 11, the half-etched PZT cavity has an etch depth of 48 μm and a surface roughness (R_a) of 0.82 μm. The over-etched PZT cavity has an etch depth of 106 μm and a surface roughness (R_a) of 0.44 μm. The undercut ratio was 0.67 for the half-etched PZT and 0.83 for the over-etched PZT.

The etched PZT surface profile was also measured by an optical profilometer (Bruker, contour GT-I) to further evaluate the surface roughness. The 3D profile is shown in Fig. 12, where the calculated arithmetical mean height (S_a) is about 0.78 μm for the etching with HBF_4:H_2O volume ratio of 1:20. This roughness is consistent with the relatively large grain sizes of ceramic PZT.

VI. Conclusion

A one-step residue-free wet etching process for ceramic PZT using diluted HBF_4 has been developed. A moderate etch rate (1.54 μm/min) and low undercut (0.78:1) are achieved at a medium volume ratio (HBF_4:H_2O=1:10). The experimental results have also demonstrated that using this wet etching process no ultrasonic agitation is needed, no residues are observed and the selectivity to photoresist is high. This simple and effective ceramic PZT etching process will greatly accelerate the development of more high-performance ceramic PZT-based MEMS devices such as microspeakers and pMUTs.

Acknowledgement

This work is sponsored by the National Institutes of Health (NIH) under the award# R01EB020601.

Biography

Haoran Wang received his B.E. degree in Measuring and Control Technology and Instruments from Tianjin University, Tianjin, China, in 2017. He is currently working toward a Ph.D. degree in the Department of Electrical and Computer Engineering at University of Florida, Gainesville, USA. His research interests include microelectromechanical (MEMS) systems, micro/nano fabrication, and piezoelectric transducers.

Manish Godara received his bachelor's degree in Chemical Engineering from Malaviya National Institute of technology (MNIT), Jaipur, India, in 2017. He is a graduate student [master's degree] in the department of Chemical Engineering at University of Florida, Gainesville, USA. He is currently working towards his internship at Micron Technology, Virginia, USA. His research interest includes microelectromechanical (MEMS) systems, wet process and heterogenous catalysis.

Zhenfang Chen, founder of MEMS Engineering & Material which develops and manufactures SOI wafers and other bonded material for MEMS and semiconductor applications. Prior to this, he worked as the principle engineer for Fujifilm Dimatix, Santa Clara, California. He received Ph.D. in metallurgical physical chemistry from Central South University, Changsha, China.

Huikai Xie received his B.S., M.S. and Ph.D. degrees in electrical and computer engineering from Beijing Institute of Technology, Tufts University and Carnegie Mellon University, respectively. He joined the University of Florida in 2002 as an assistant professor, where he is currently a professor at the Department of Electrical and Computer Engineering. He also worked at Tsinghua University as a researcher, Robert Bosch Company as a summer intern, and US Air Force Research Lab as a summer faculty fellow. His research interests include MEMS/NEMS, integrated sensors, microactuators, integrated power passives, CNT-CMOS integration, optical MEMS, LiDAR, micro-spectrometers, optical bioimaging, and endomicroscopy. He is an associate editor of IEEE Sensors Letters, and Sensors & Actuators A. He has published over 300 technical papers and holds more than 30 patents. He is a fellow of IEEE and SPIE.

References

[1]. Pulskamp JS, Rudy RQ, Bedair SS, Puder JM, Breen MG and Polcawich RG, "Ferroelectric PZT MEMS HF/VHF resonators/filters," 2016 IEEE International Frequency Control Symposium (IFCS), New Orleans, LA, 2016, pp. 1–4.

[2]. Zhu Y, Liu W, Jia K, Liao W, and Xie H, "A piezoelectric unimorph actuator based tip-tilt-piston micromirror with high fill factor and small tilt and lateral shift," Sensors and Actuators, A: Physical, vol. 167, no. 2, pp. 495–501, 2011.

[3]. Grinberg I, Maccabi N, Kassie A, and Elata D, "A piezoelectric twisting beam actuator," Journal of Microelectromechanical Systems, vol. 26, no. 6, pp. 1279–1286, 2017.

[4]. Kanda T, Makino A, Ono T, Suzumori K, Morita T, and Kurosawa MK, "A micro ultrasonic motor using a micro-machined cylindrical bulk PZT transducer," Sensors and Actuators, A: Physical, vol. 127, no. 1, pp. 131–138, 2006.

[5]. Kim HJ, Yang WS, and No K, "Improvement of low-frequency characteristics of piezoelectric speakers based on acoustic diaphragms," IEEE Transactions on Ultrasonics, Ferroelectrics, and Frequency Control, vol. 59, no. 9, pp. 2027–2035, 2012.

[6]. Zhou Z, Yoshida S, and Tanaka S, "Epitaxial PMnN-PZT/Si MEMS ultrasonic rangefinder with 2 m range at 1 V drive," Sensors and Actuators, A: Physical, vol. 266, pp. 352–360, 2017.

[7]. Liao W. Piezoelectric micromachined ultrasound transducer array for photoacoustic imaging; The 13th International Conference on Solid-State Sensors, Actuators and Microsystems; 2013. 1831–1834.

[8]. Perçin G, Atalar A, Degertekin F. Levent, and Khuri-Yakub BT, "Micromachined two-dimensional array piezoelectrically actuated transducers," Applied Physics Letters, vol. 72, no. 11, pp. 1397–1399, 1998.

[9]. Brodal E, Melands F, and Jacobsen S, "Performance of an ultrasonic imaging system based on a 45-MHz linear PVDF transducer array: A numerical study," Advances in Acoustics and Vibration, vol. 2011, pp. 1–15, 2011.

[10]. Cho IJ, Jang S, and Nam HJ, "A piezoelectrically actuated MEMS speaker with polyimide membrane and thin film Pb(Zr,Ti)O_3(PZT) actuator," Integrated Ferroelectrics, vol. 105, no. 1, pp. 27–36, 2009.

[11]. Moreira M, Bjurström J, Katardjev I, and Yantchev V, "Aluminum scandium nitride thin-film bulk acoustic resonators for wide band applications," Vacuum, vol. 86, no. 1, pp. 23–26, 2011.

[12]. Calame F and Muralt P, "Growth and properties of gradient free sol-gel lead zirconate titanate thin films," Applied Physics Letters, vol. 90, 062907, 2007.

[13]. Yeo HG, Xue T, Roundy S, Ma X, Rahn C and Trolier-McKinstry S, "Strongly (001) oriented bimorph PZT film on metal foils grown by rf-sputtering for wrist-worn piezoelectric energy harvesters," Advanced Functional Materials, vol. 28, no. 1801327, pp. 1–9, 2018.

[14]. Wang Z, Miao J, Tan CW and Xu T, "Fabrication of piezoelectric MEMS devices from thin film to bulk PZT wafer," Journal of Electroceramics, vol. 24, pp. 25–32, 2010.

[15]. Muralt P, "Ferroelectric thin films for micro-sensors and actuators: a review," Journal of Micromechanics and Microengineering, vol. 10, pp. 136–146, 2000.

[16]. Hareesh P, Misri I, Yang S, and DeVoe DL, "Transverse interdigitated electrode actuation of homogeneous bulk PZT," Journal of Microelectromechnical Systems, vol. 21, no. 6, pp. 1513–1518, 2012.

[17]. Aktakka EE, Peterson RL, and Najafi K, "A CMOS-compatible piezoelectric vibration energy scavenger based on the intergation of bulk PZT films on silicon," 2010 Internation Electron Device Metting (IEDM), 2010, pp. 31.5.1–31.5.4.

[18]. Wang Z, Miao J, and Tan CW, "Acoustic transducers with a perforated damping backplate based on PZT/silicon wafer bonding technique," Sensors and Actuators, A: Physical, vol. 149, no. 2, pp. 277–283, 2009.

[19]. Wang H, Yu Y, Chen Z, Yang H, Jiang H and Xie H, "Design and fabrication of a piezoelectric micromachined ultrasonic transducer array based on ceramic PZT," IEEE Sensors Conference, 2018.

[20]. Jung JK and Lee WJ, "Dry etching characteristics of $Pb(Zr,Ti)O_3$ films in CF_4 and Cl_2/CF_4 inductively coupled plasmas," Japanese Journal of Applied Physics, Part 1: Regular Papers and Short Notes and Review Papers, vol. 40, no. 3 A, pp. 1408–1419, 2001.

[21]. Miller RA and Bernstein JJ, "A novel wet etch for patterning lead zirconate-titanate (PZT) thin-films," Integrated Ferroelectrics, vol. 29, pp. 225–231, 2000.

[22]. Zheng K, Lu J, and Chu J, "A novel wet etching process of $Pb(Zr,Ti)O_3$ thin films for applications in microelectromechanical system," Japanese Journal of Applied Physics, Part 1: Regular Papers and Short Notes and Review Papers, vol. 43, no. 6 B, pp. 3934–3937, 2004.

[23]. Baborowski J, "Microfabrication of piezoelectric MEMS," Journal of Electroceramics, vol. 12, pp. 33–51, 2004.

[24]. Mancha S, "Chemical etching of thin film PLZT," Ferroelectrics, vol. 135, no. 1, pp. 131–137, 1992.

[25]. Xu XH, Li BQ, Feng Y, and Chu JR, "Design, fabrication and characterization of a bulk-PZT-actuated MEMS deformable mirror," Journal of Micromechanics and Microengineering, vol. 17, no. 12, pp. 2439–2446, 2007.

[26]. Aktakka EE, Peterson RL, and Najafi K, "A 3-DOF Piezoelectric Micro Vibratory Stage Based on Bulk-PZT/Silicon Crab-Leg Suspensions," 2013 IEEE 26th International Conference on Micro Electro Mechanical Systems (MEMS), 2013, pp. 576–579.

[27]. Wang S, Ma B, Deng J, Qu H, and Luo J, "Fabrication and characterization of MEMS piezoelectric synthetic jet actuators with bulk-micromachined PZT thick film," Microsystem Technologies, vol. 21, no. 5, pp. 1053–1059, 2015.

[28]. Wang L-P, Wolf R, Zhou Q, Trolier-McKinstry S, and Davis RJ, "Wet-Etch Patterning of Lead Zirconate Titanate (PZT) Thick Films for Microelectromechanical Systems (MEMS) Applications," MRS Proceedings, vol. 657, p. EE5.39, 2000.

[29]. Che L, Halvorsen E, and Chen X, "An optimized one-step wet etching process of $Pb(Zr_{0.52}Ti_{0.48})O_3$ thin films for microelectromechanical system applications." Journal of Micromechanics and Microengineering, vol. 21, no. 10, 2011.

[30]. Ross PJ, Taguchi Techniques for Quality Engineering: Loss Function, Orthogonal Experiments, Parameter and Tolerence Design, Mc Graw Hill, New York, 1988.

Highlights

- A new wet etching recipe for ceramic PZT, which consists of only one acid, does not require ultrasonic agitation, and does not generate residues, has been developed.
- Taguchi design of experiments (DOE) method is employed to minimize the number of etching experiments.
- Experimental results have demonstrated that high etch rate, small undercut, no residues and high selectivity can be simultaneously achieved without using any ultrasonic agitation, which is critical for making high-performance piezoelectric MEMS devices based on adhesive-bonded ceramic PZT.
- Etch rates with different acid concentrations, stirring speeds and temperatures are experimentally obtained and plotted in the paper, which can be adopted for various etching purposes.

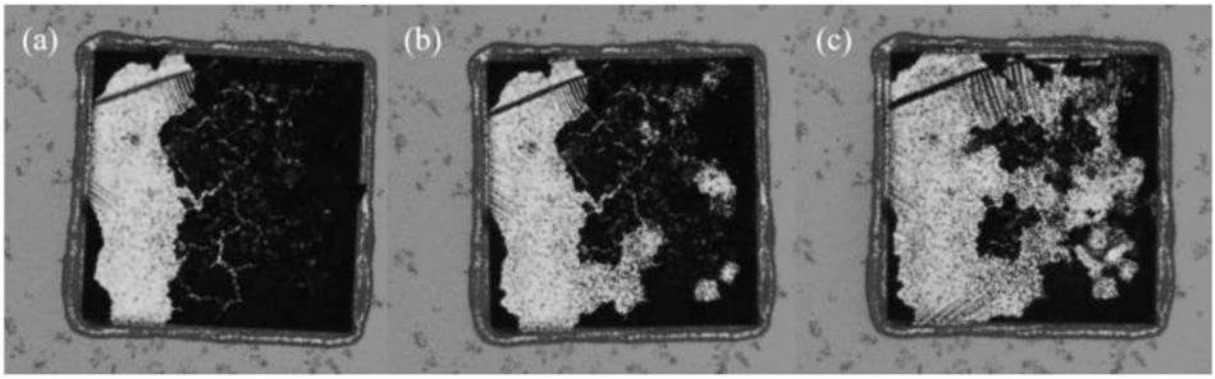

Fig. 1.

Residues remained after etching (a). Residues were partially removed after dipped in heated DI water (b) and rinsed with DI water gun (c).

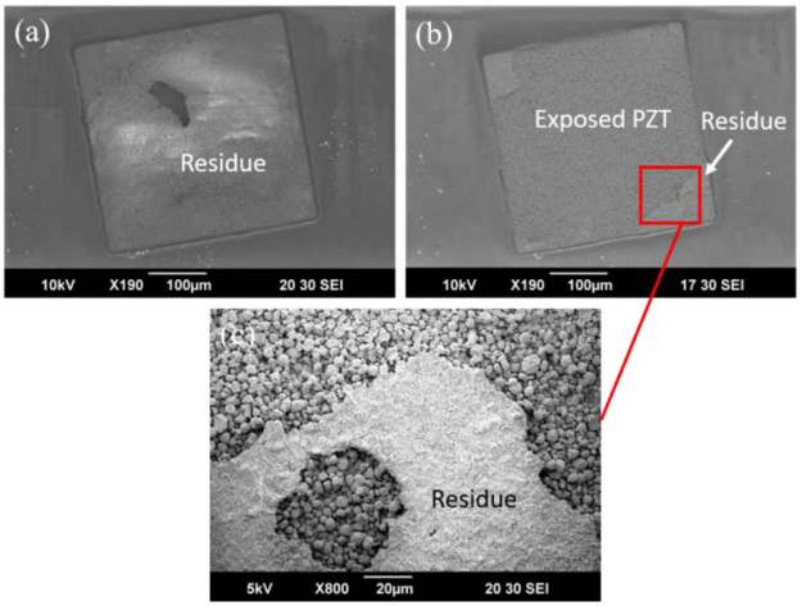

Fig. 2.

SEM of the etched PZT pattern with residues remained after etching (a) and removed after 10s ultrasonic cleaning (b). Zoom-in SEM of residues and exposed PZT (c).

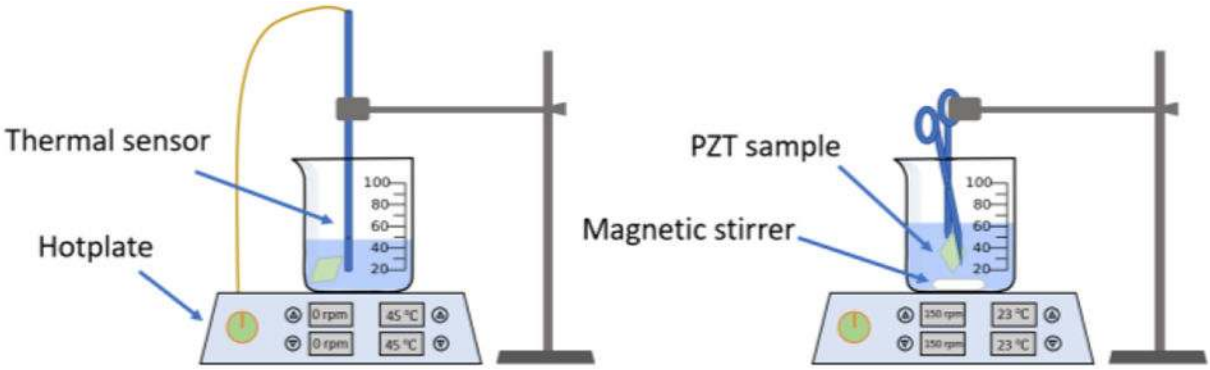

Fig. 3.
Schematic of the experimental setup.

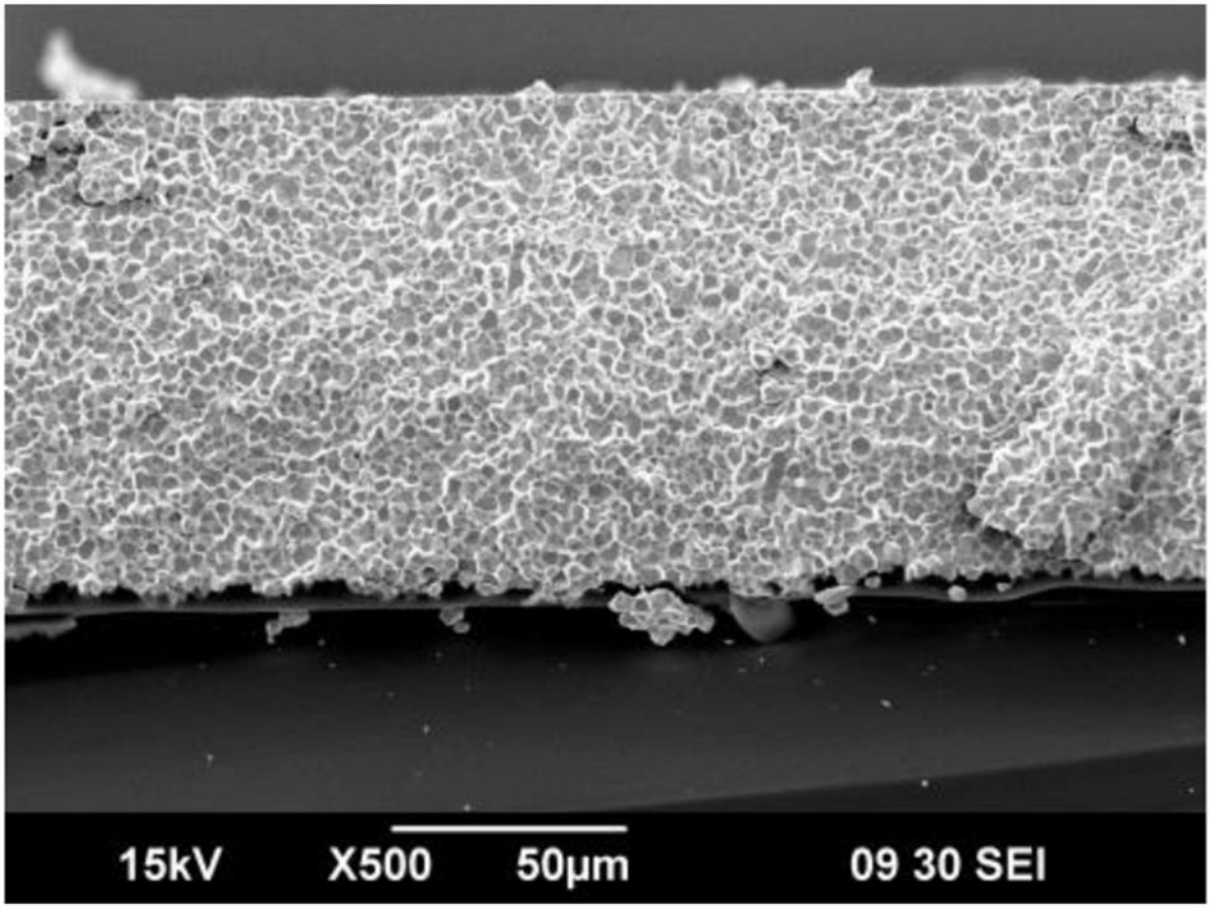

Fig. 4.
SEM of a polished ceramic PZT in cross view.

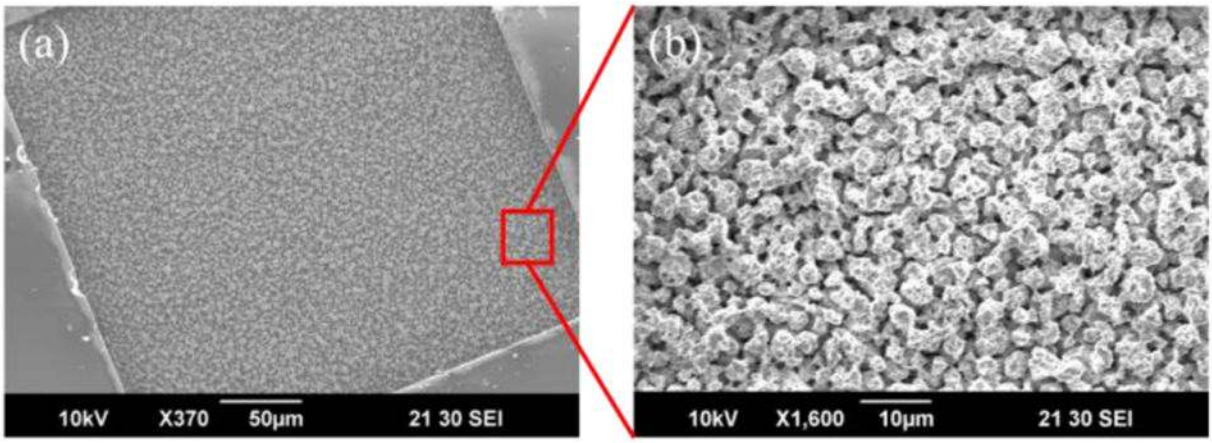

Fig. 5.
SEM of the etched PZT pattern (a) and PZT grains (b).

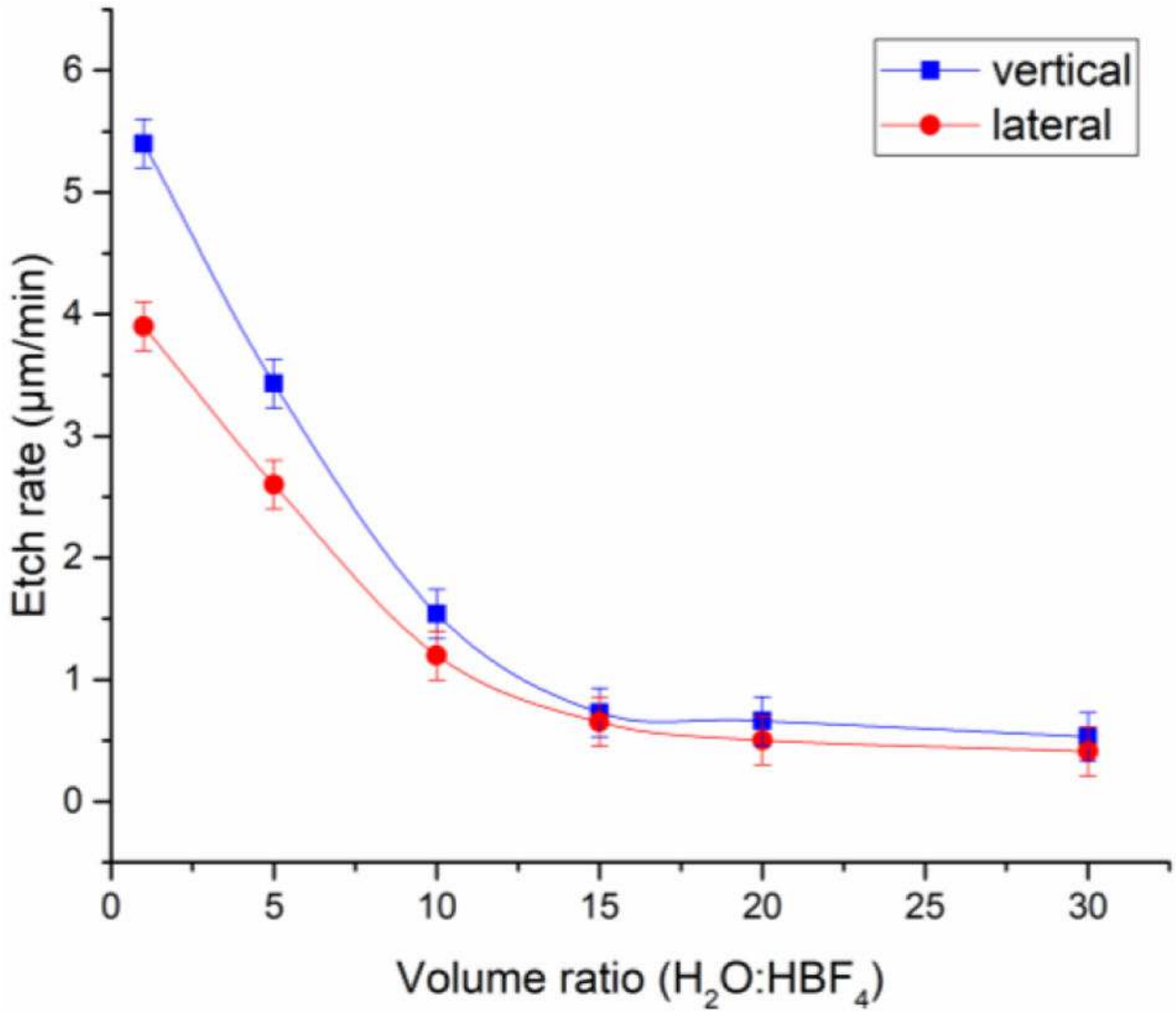

Fig. 6.
Vertical and lateral etch rates vs. acid concentrations in room temperature.

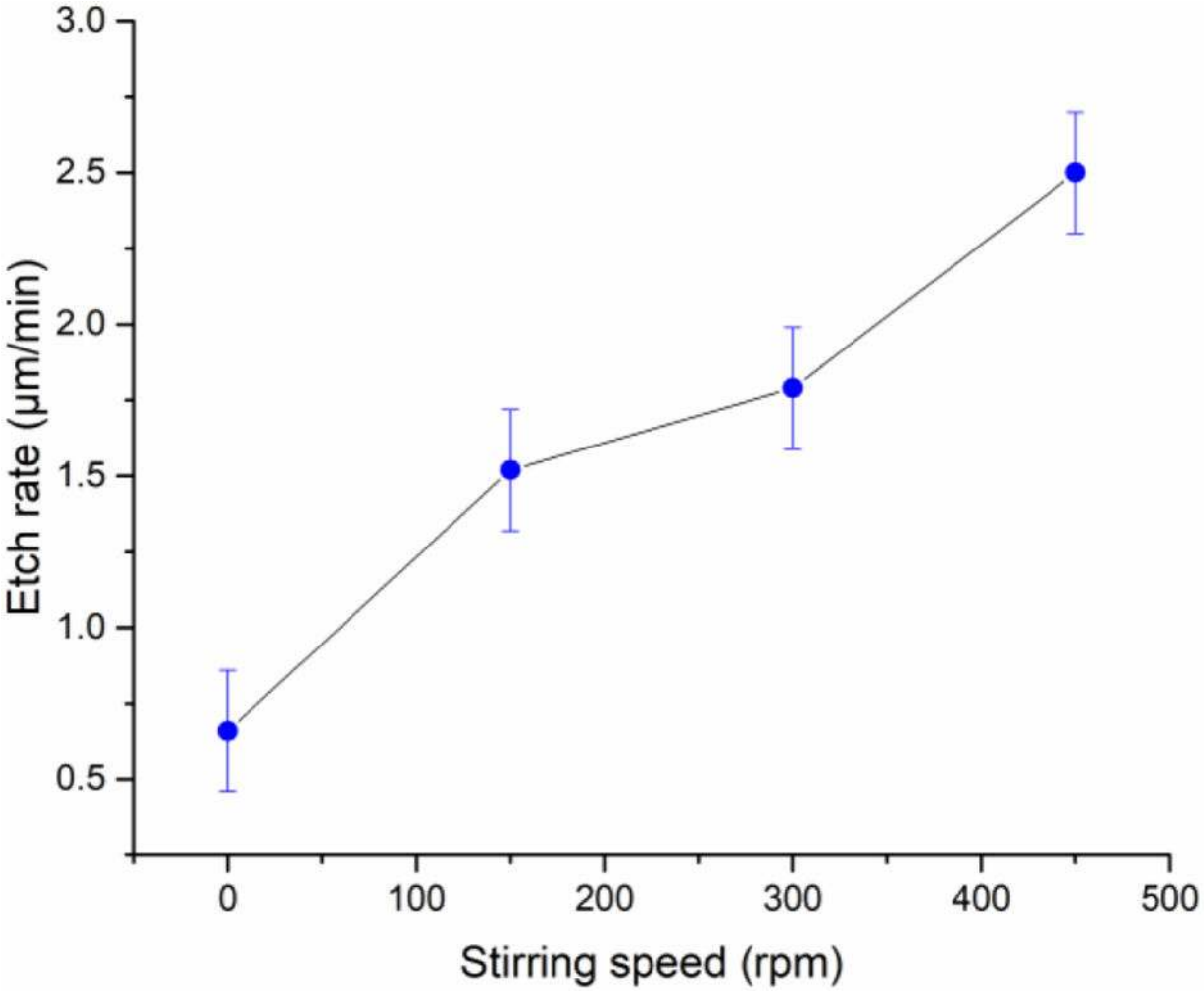

Fig. 7.
Vertical etch rate vs. stirring speed in room temperature.

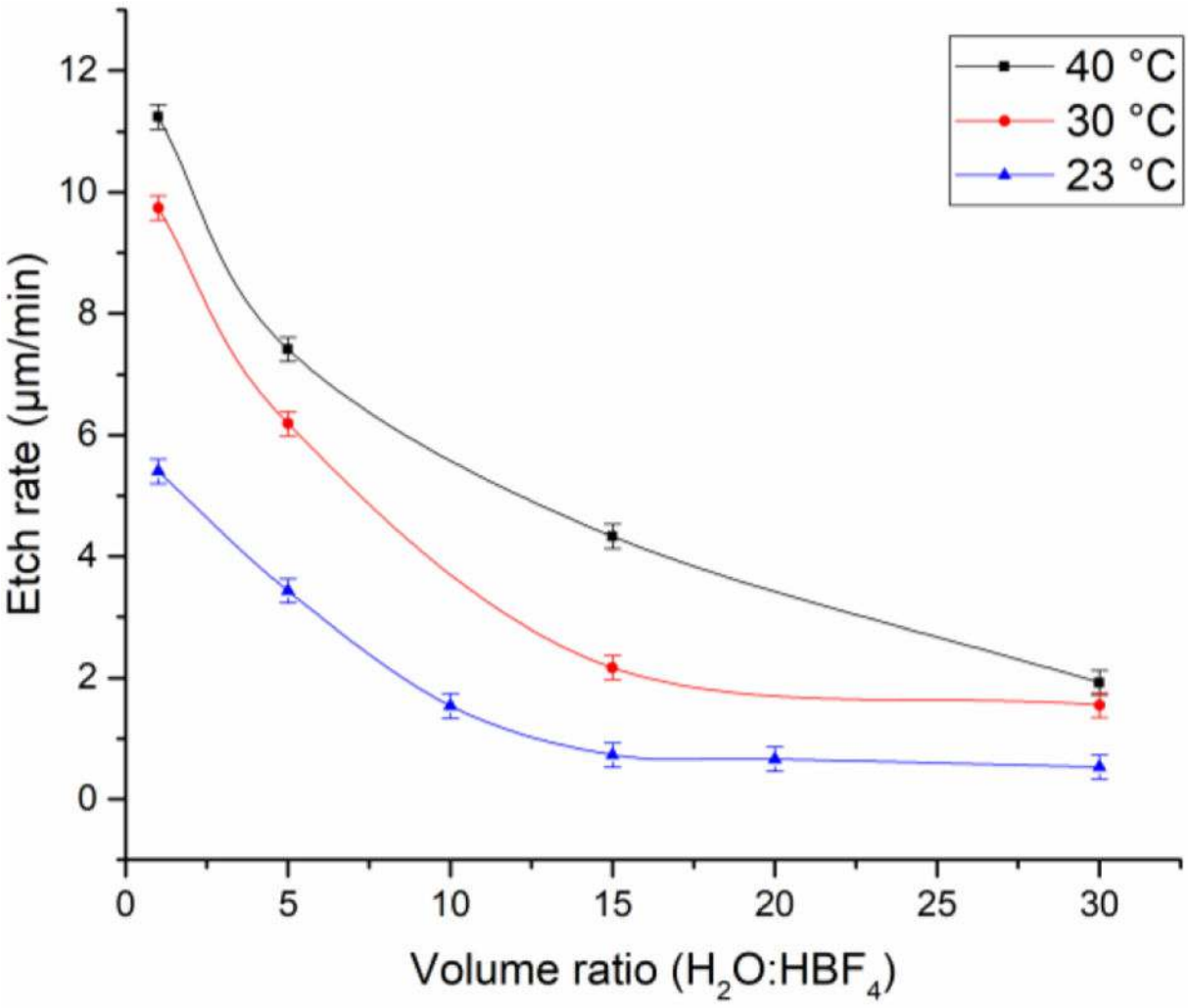

Fig. 8.
Vertical etch rate vs. acid concentration with different temperatures.

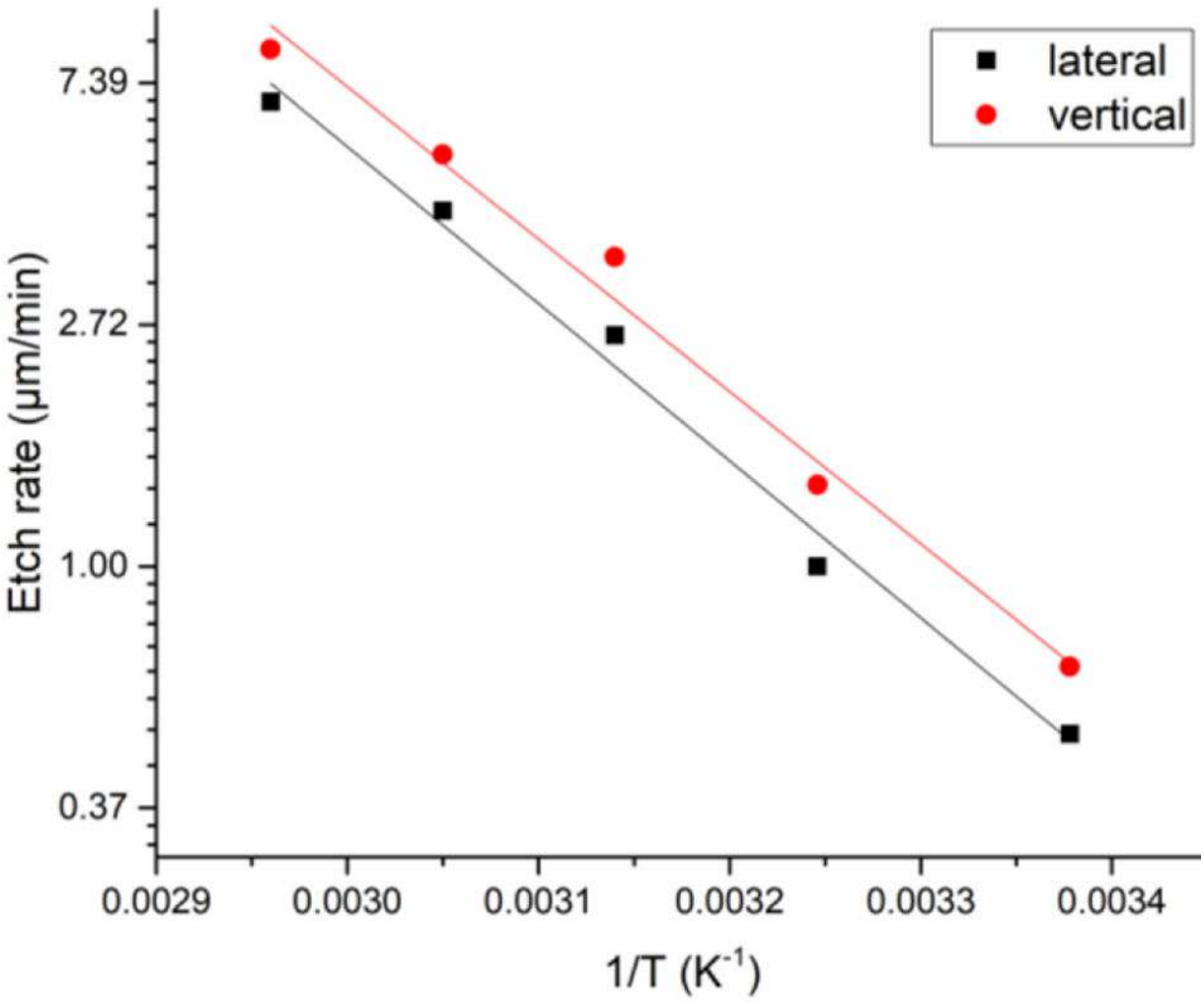

Fig. 9.
Linear fitted results of etch rate vs. 1/T.

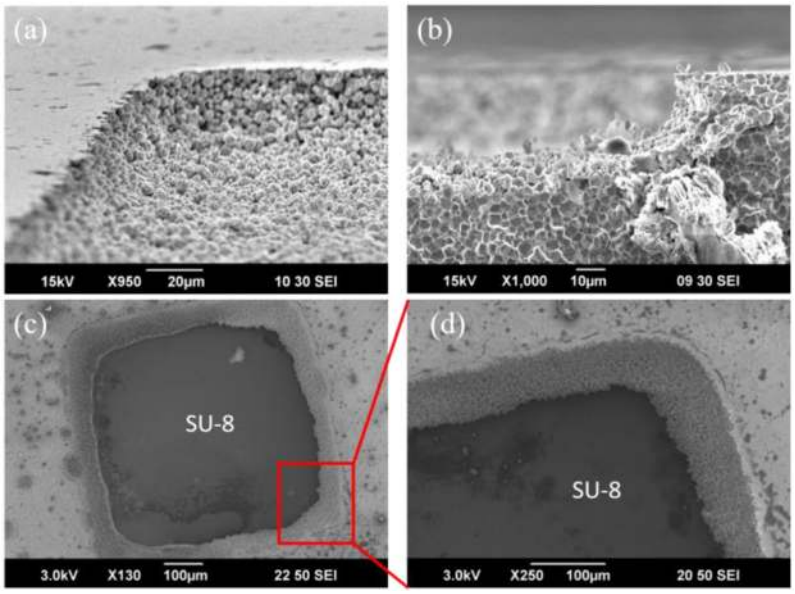

Fig. 10.

SEM images of the sidewall (a) and the cross view (b) of a moderately etched cavity, the top view (c) and sidewall (d) of an over etched cavity.

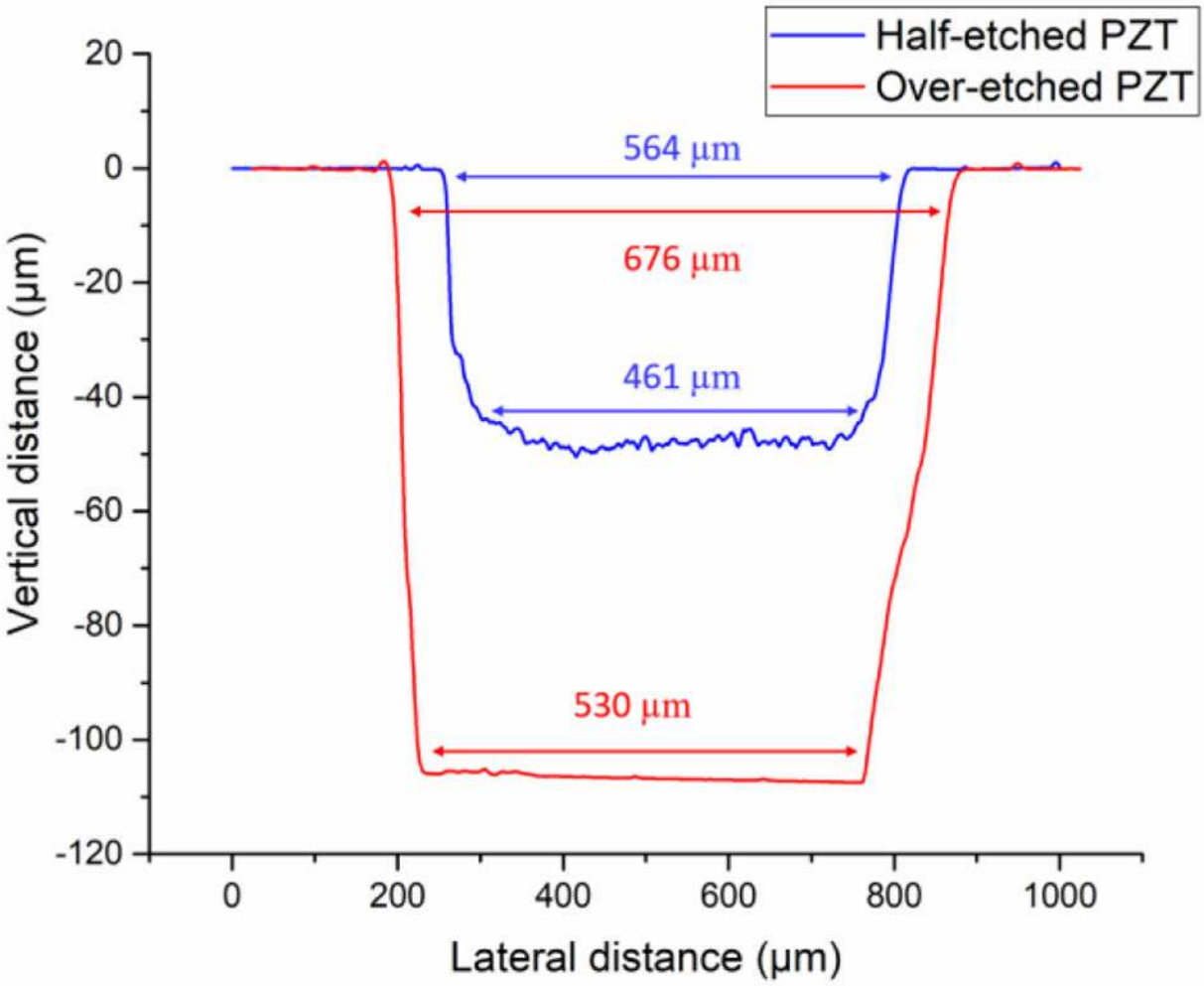

Fig. 11.
Etched profiles of PZT cavities measured by the surface profilometer.

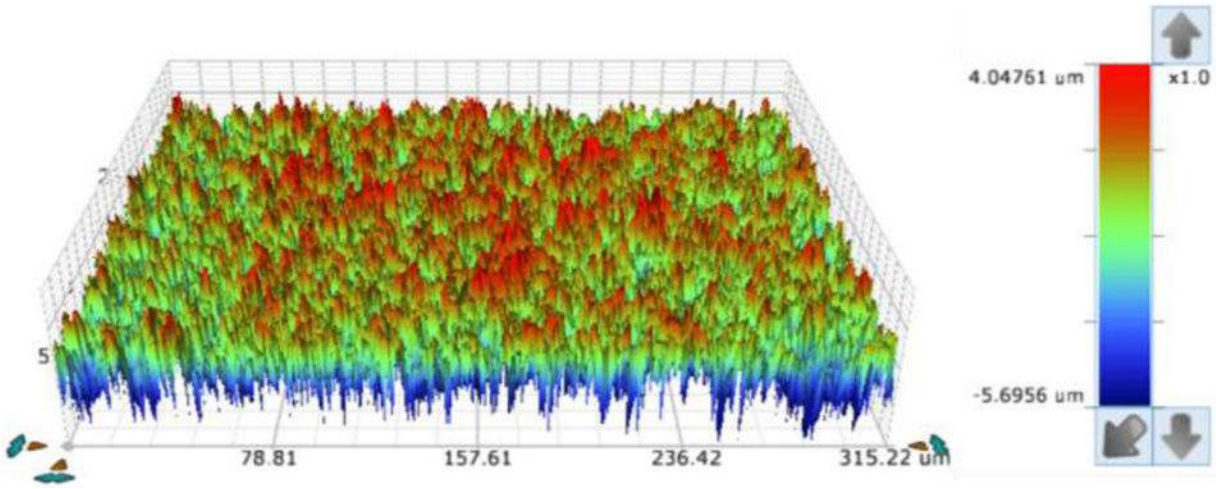

Fig. 12.
3D image of the etched surface profile.

Table I

Design parameters and their levels in the experiment.

Factor	Temperature (°C)	Volume ratio (HBF_4:H_2O)	Agitation
Level 1	23	1:10	None
Level 2	40	1:1	Vibration
Level 3	60	1:0	Ultrasound

Table II

Experiments designed based on an L9 orthogonal array.

Trial #	Temperature (°C)	Volume ratio (HBF_4:H_2O)	Agitation
1	23	1:10	None
2	23	1:1	Vibration
3	23	1:0	Ultrasound
4	40	1:10	Vibration
5	40	1:1	Ultrasound
6	40	1:0	None
7	60	1:10	Ultrasound
8	60	1:1	None
9	60	1:0	Vibration

Table III

Experimental results.

#	Temperature (°C)	Volume ratio (HBF_4:H_2O)	Agitation	Etch rate (vertical)/ μm/min	Undercut	
					Rate (μm/min)	Ratio
1	23	1:10	None	1.5	1.2	0.80
2	23	1:1	Vibration	5.9	4.7	0.80
3	23	1:0	Ultrasound	0.4	2.6	6.50
4	40	1:10	Vibration	8.6	5.2	0.60
5	40	1:1	Ultrasound	27.2	19.2	0.71
6	40	1:0	None	0.5	2.0	4.00
7	60	1:10	Ultrasound	21.3	16.6	0.78
8	60	1:1	None	7.4	4.8	0.65
9	60	1:0	Vibration	1.3	4.0	3.08

Table IV

Mean values of each level of design parameters.

Parameter	level	temperature	Volume ratio	Agitation
Etch rate (vertical)	1	2.6	10.5	3.1
	2	12.1	13.5	5.3
	3	10	0.7	16.3
	S	4.99	6.69	7.04
	Rank	3	2	1
Undercut (lateral)	1	2.8	7.7	2.7
	2	8.8	9.6	4.6
	3	8.5	2.9	12.8
	S	3.38	3.45	5.37
	Rank	3	2	1